Electronic Supplementary Material (ESI) for Journal of Materials Chemistry C.

White light Emission of IFP-1 by In-situ Co-doping of the MOF Pore System with with Eu^{3+} and Tb^{3+}

Suvendu Sekhar Mondal,[a] Karsten Behrens [a] Philipp R. Matthes,[b] Fabian Schönfeld,[b] Jörn Nitsch,[b] Andreas Steffen,[b] Philipp-Alexander Primus,[c] Michael U. Kumke,[c] Klaus Müller-Buschbaum[,b] Hans-Jürgen Holdt*[,a]*

[a]Institut für Chemie, Anorganische Chemie, Universität Potsdam, Karl-Liebknecht-Straße 26, 14476 Golm, Germany

[b]Institut für Anorganische Chemie, Universität Würzburg, Am Hubland, 97074 Würzburg, Germany

[c]Institut für Chemie, Physikalische Chemie, Universität Potsdam, Karl-Liebknecht-Str. 25, 14476 Golm, Germany

Table of Content

1. IR-spectroscopy, elemental analysis and ICP-OES:

IR spectra were recorded on FT-IR Nexus from Thermo Nicolet in the region of 4000 – 400 cm^{-1} using KBr pellets. Elemental analysis (C, H, N) was performed on Elementar Vario EL elemental analyzer. . ICP-OES measurements was performed on the Perkin Elmer Optical Emission Spectrometer Optima 5300 DV (Scott-Chamber/Cross-Flow-Nebulizer). Zn was observed at λ = 213.8 nm, Eu at λ = 412.9 nm and Tb at λ = 350.9 nm.

Eu@IFP-1-*a*: Yield: 80% based on $Zn(NO_3)_2 \cdot 4H_2O$; Elemental analysis: for $C_6H_6N_4O_2Zn_1$ = IFP-1; calcd (%): C 31.12, H 2.61, N 24.2, Zn 28.24; found: C 31.15, H 2.60, N 22.62, Zn 28.47; MIR (KBr pellet): (3337 m, 3266 m, 3119 m, 1659 s, 1550 vs, 1461 m, 1436 m, 1261 m, 1114 m, 810 m) cm^{-1}.

Eu@IFP-1-*b*: Yield: 70% based on $Zn(NO_3)_2 \cdot 4H_2O$; Elemental analysis: $C_{6.00}H_{6.00}N_{4.00}O_{2.00}Zn_1Eu_{0.0003}$ = IFP-1 · 0.0003 $Eu(HCO_2)_3$; calcd (%): C 31.12, H 2.61, N 24.19, Zn 28.24, Eu 0.02; found: C 31.41, H 2.62, N 23.99, Zn 28.26, Eu 0.02; MIR (KBr pellet): (3337 m, 3266 m, 3119 m, 1659 s, 1550 vs, 1462 m, 1436 m, 1264 m, 1114 m, 810 m) cm^{-1}.

Eu@IFP-1-*c*: Yield: 63% based on $Zn(NO_3)_2 \cdot 4H_2O$; Elemental analysis: $C_{6.01}H_{6.01}N_{4.00}O_{2.03}Zn_1Eu_{0.005}$ = IFP-1 · 0.005 $Eu(HCO_2)_3$; calcd (%): C 30.99, H 2.60, N 24.05, Zn 28.08, Eu 0.33; found: C 30.28, H 2.50, N 22.64 Zn 28.15, Eu 0.25; MIR (KBr pellet): (3343 m, 3281 m, 3119 m, 1662 s, 1553 vs, 1461 m, 1437 m, 1265 m, 1114 m, 811 m) cm^{-1}.

Eu@IFP-1-*d*: Yield: 70% based on $Zn(NO_3)_2 \cdot 4H_2O$; Elemental analysis: $C_{6.03}H_{6.03}N_{4.00}O_{2.06}Zn_1Eu_{0.01}$ = IFP-1 · 0.01 $Eu(HCO_2)_3$; calcd (%): C 30.90, H 2.59, N 23.90, Zn 27.90, Eu 0.65; found: C 30.86, H 2.63, N 23.32, Zn 28.31, Eu 0.69 MIR (KBr pellet): (3337 m, 3257 m, 3119 m, 1660 s, 1549 vs, 1462 m, 1435 m, 1264 m, 1114 m, 810 m) cm^{-1}.

Tb@IFP-1-*a*: Yield: 75% based on $Zn(NO_3)_2 \cdot 4H_2O$; Elemental analysis: $C_{6.00}H_{6.50}N_{4.00}O_{2.25}Zn_{1.00}Tb_{0.0007}$ = IFP-1 · 0.0007 $Tb(HCO_2)_3$ · 0.25 H_2O; calcd (%) C 30.51, H 2.77, N 23.71, Zn 27.69, Tb 0.05; found: C 30.22, H 2.47, N 23.45, Zn 28.26, Tb 0.05; MIR (KBr pellet): (3343 m, 3279 m, 3119 m, 1661 s, 1551 vs, 1461 m, 1437 m, 1265 m, 1114 m, 810 m) cm^{-1}.

Tb@IFP-1-*b*: Yield: 64% based on $Zn(NO_3)_2 \cdot 4H_2O$; Elemental analysis: $C_{6.00}H_{6.00}N_{4.00}O_{2.01}Zn_{1.00}Tb_{0.001}$ = IFP-1 · 0.001$Tb(HCO_2)_3$ · 0.50 H_2O; calcd (%): C 29.95, H 2.93, N 23.28, Zn 27.17, Tb 0.03; found: C 29.53, H 2.63, N 23.14, Zn 27.47, Tb 0.06; MIR (KBr pellet): (3343 m, 3280 m, 3119 m, 1661 s, 1551 vs, 1461 m, 1438 m, 1265 m, 1114 m, 811 m) cm^{-1}.

Tb@IFP-1-*c*: Yield: 57% based on $Zn(NO_3)_2 \cdot 4H_2O$; Elemental analysis: $C_{6.00}H_{6.50}N_{4.00}O_{2.26}Zn_{1.00}Tb_{0.0008}$ = IFP-1 · 0.0008$Tb(HCO_2)_3$ · 0.25 H_2O; calcd (%): C 30.51, H 2.77, N 23.71, Zn 27.68, Tb 0.05; found: C 30.28, H 2.53, N 22.51, Zn 27.58, Tb 0.05; MIR (KBr pellet): (3343 m, 3275 m, 3119 m, 1661 s, 1551 vs, 1461 m, 1438 m, 1265 m, 1114 m, 811 m) cm^{-1}.

Tb@IFP-1-*d*: Yield: 64% based on $Zn(NO_3)_2 \cdot 4H_2O$; Elemental analysis: $C_{6.00}H_{7.05}N_{4.00}O_{2.51}Zn_{1.00}Tb_{0.001}$ = IFP-1 · 0.001$Tb(HCO_2)_3$ · 0.50 H_2O; calcd (%): C 29.94, H 2.93, N 23.26, Zn 27.16, Tb 0.07; found: C 29.44, H 2.59, N 22.97, Zn 27.74, Tb 0.11; MIR (KBr pellet): (3343 m, 3279 m, 3119 m, 1661 s, 1550 vs, 1461 m, 1438m, 1265 m, 1114 m, 811 m) cm^{-1}.

EuTb@IFP-1-*a*: Yield: 69% based on $Zn(NO_3)_2{\cdot}4H_2O$; Elemental analysis: $C_{6.00}H_{6.00}N_{4.00}O_{2.00}Zn_{1.00}Eu_{0.0003}Tb_{0.0003}$ = IFP-1 · 0.0006EuTb$(HCO_2)_3$; calcd (%): C 31.11, H 2.61, N 24.18, Zn 28.23, Eu 0.01, Tb 0.01; found: C 30.42, H 2.50, N 23.58, Zn 28.00, Eu0.02, Tb 0.02; MIR (KBr pellet): (3340 m , 3275 m, 3127 m, 1666 s, 1560 vs, 1461 m, 1438 m, 1266 m, 1115 m, 813 m) cm^{-1}.

EuTb@IFP-1-*b*: Yield: 66% based on $Zn(NO_3)_2{\cdot}4H_2O$; Elemental analysis: $C_{6.00}H_{6.00}N_{4.00}O_{2.01}Zn_{1.00}Eu_{0.0006}Tb_{0.0006}$ = IFP-1 · 0.0012EuTb$(HCO_2)_3$; calcd (%): C 31.09, H 2.61, N 24.16, Zn 28.21, Eu 0.04, Tb 0.04; found: C 31.02, H 2.56, N 23.19, Zn 28.26, Eu0.04, Tb 0.05; MIR (KBr pellet): (3341 m, 3275 m, 3129 m, 1665 s, 1562 vs, 1462 m, 1440 m, 1266 m, 1116 m, 813 m) cm^{-1}.

EuTb@IFP-1-*c*: Yield: 64% based on $Zn(NO_3)_2{\cdot}4H_2O$; Elemental analysis: $C_{6.06}H_{6.06}N_{4.00}O_{2.12}Zn_{1.00}Eu_{0.01}Tb_{0.01}$ = IFP-1 · 0.02EuTb$(HCO_2)_3$; calcd (%): C 30.66, H 2.57, N 23.60, Zn 27.56, Eu 0.64, Tb 0.67; found: C 30.54, H 2.35, N 22.78, Zn 27.62, Eu 0.59, Tb 0.62; MIR (KBr pellet): (3346 m, 3280 m, 3127 m, 1659 s, 1564 vs, 1464 m, 1439 m, 1266 m, 1115 m, 812 m) cm^{-1}.

EuTb@IFP-1-*d*: Yield: 64% based on $Zn(NO_3)_2{\cdot}4H_2O$; Elemental analysis: $C_{6.42}H_{6.92}N_{4.00}O_{3.09}Zn_{1.00}Eu_{0.07}Tb_{0.07}$ = IFP-1 · 0.14EuTb$(HCO_2)_3$ · 0.25 H_2O; calcd (%): C 27.87, H 2.52, N 20.25, Zn 23.64, Eu 3.84, Tb 4.02; found: C 28.22, H 2.58, N 20.70, Zn 22.23, Eu 3.98, Tb 3.93; MIR (KBr pellet): (3345 m, 3280 m, 3126 m, 1665 s, 1564 vs, 1464 m, 1439 m, 1267 m, 1115 m, 812 m) cm^{-1}.

2 Powder X-ray Diffraction (PXRD)

For X-ray powder patterns of Ln@IFP-1*a* - *d* (Ln=Eu, Tb) and EuTb@IFP-1*a* - *d* were measured on a Siemens Diffractometer D5005 in Bragg-Brentano reflection geometry. The Diffractometer was equipped with a copper tube, a scintillation counter, with stepper motor controlled variable slits on both primary and diffracted beams (automatical incident- and diffracted-beam soller slits) and with a graphite secondary monochromator. The generator was set to 40 kV and 40 mA with using Cu K-alpha radiation (1.54056 Å). All measurements were performed with sample rotating. Data were collected digitally from 3° to 70° 2θ using a step size of 0.02° 2θ and a count time of 4 seconds per step.

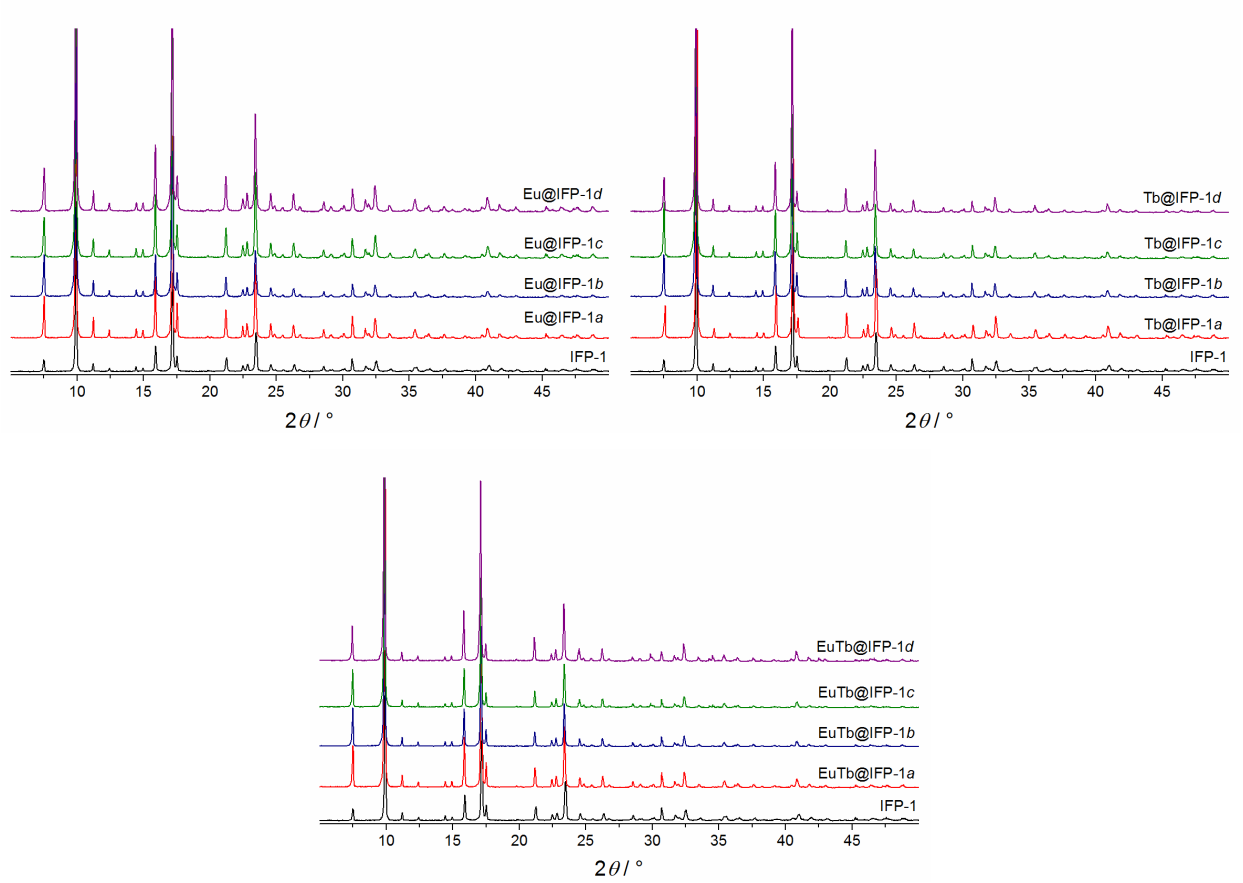

Fig. S01. Powder X-ray diffraction patterns of IFP-1 and of Ln@IFP-1 materials. Cu-K_α radiation (λ=1.54056 Å).

3 SEM – Scanning Electron Microscopy and EDX - Energy-dispersive X-ray spectroscopy

SEM-/EDX measurements was done on a JEOL JSM 6510 SEM equipped with an EDX spectrometer of Oxford (INCAx-act SN detector). For measurements all samples were activated under vacuum by 200 °C for two days and then coated with carbon (POLARON CC7650 Carbon Coater).

3.1 Eu@IFP-1

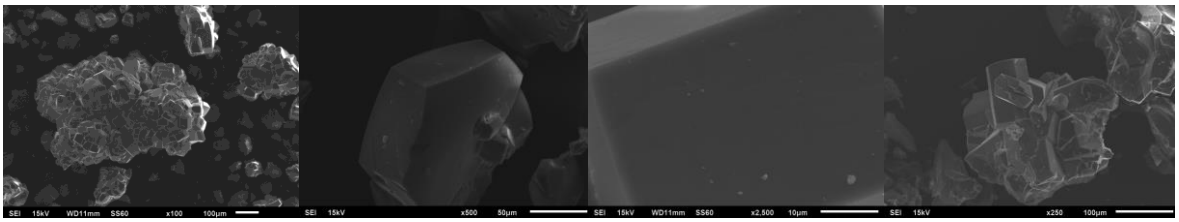

Fig. S02. SEM images of Eu@IFP-1*a*-*d*.

3.2 Tb@IFP-1

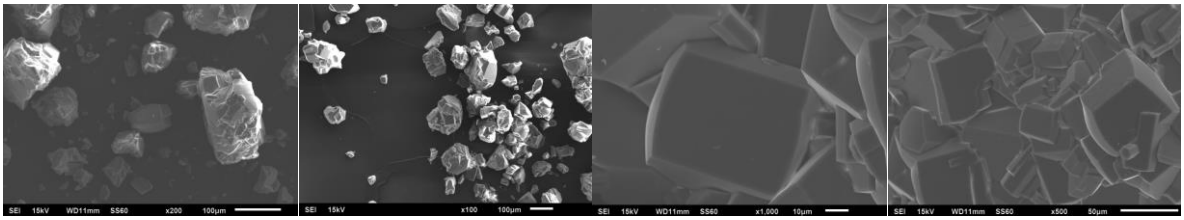

Fig. S03. SEM images of Tb@IFP-1*a* - *d*.

3.3 EuTb@IFP-1

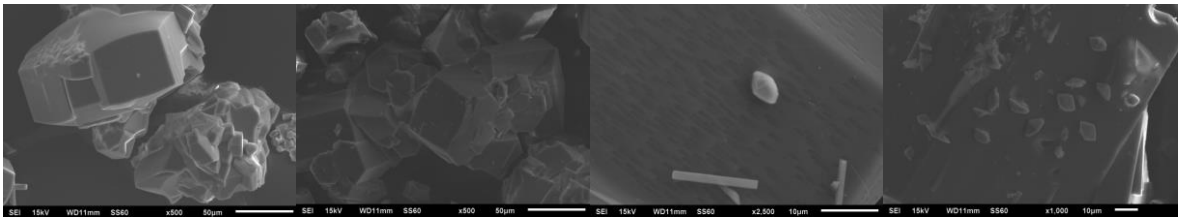

Fig. S04. SEM images of EuTb@IFP-1*a* - *d*.

Table S1. EDX results of Eu@IFP-1*a*-*d* in atom%.

Eu@IFP-1*x*	eq. $Eu(NO_3)_3 \cdot 6H_2O$	Zinc		Europium	
a	0.25	99.71	± 0.47	0.29	± 0.47
b	0.50	99.79	± 0.25	0.21	± 0.25
c	0.75	98.45	± 2.01	1.55	± 2.01
d	1.00	99.08	± 0.50	0.92	± 0.50

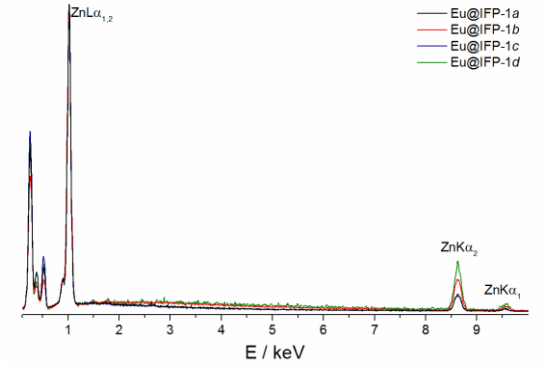

Fig. S05. Comparison of representative EDX-spectra of Eu@IFP-1*a* (black), Eu@IFP-1*b* (red); Eu@IFP-1*c* (blue); Eu@IFP-1*d* (green). All spectras are normalized to the $ZnL\alpha_{1,2}$ signal.

Table S2. EDX results of Tb@IFP-1*a*-*d* in atom%.

Tb@IFP-1*x*	eq. $Tb(NO_3)_3 \cdot 5H_2O$	Zinc		Terbium	
a	0.25	99.75	± 1.30	0.25	± 1.30
b	0.50	99.58	± 0.39	0.42	± 0.39
c	0.75	99.97	± 0.84	0.03	± 0.84
d	1.00	98.61	± 2.97	1.39	± 2.97

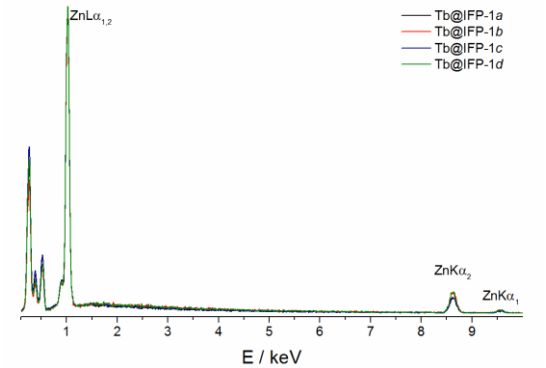

Fig. S06. Comparison of representative EDX-spectra of Tb@IFP-1*a* (black), Tb@IFP-1*b* (red); Tb@IFP-1*c* (blue); Tb@IFP-1*d* (green). All spectras are normalized to the $ZnL\alpha_{1,2}$ signal.

Table S3. EDX results of EuTb@IFP-1-*a*-*d* in atom%.

EuTb@IFP-1-x	eq. $Eu(NO_3)_3 \cdot 6H_2O$ eq. $Tb(NO_3)_3 \cdot 5H_2O$	Zinc		Europium		Terbium	
a	0.25/0.25	98.69	± 3.85	-0.52	± 4.23	1.83	± 4.12
b	0.50/0.50	99.02	± 1.15	0.25	± 0.36	0.72	± 0.65
c	0.75/0.75	97.74	± 3.20	0.93	± 1.49	1.33	± 1.78
d	1.00/1.00	71.43	± 45.51	22.12	± 22.33	23.22	± 23.20

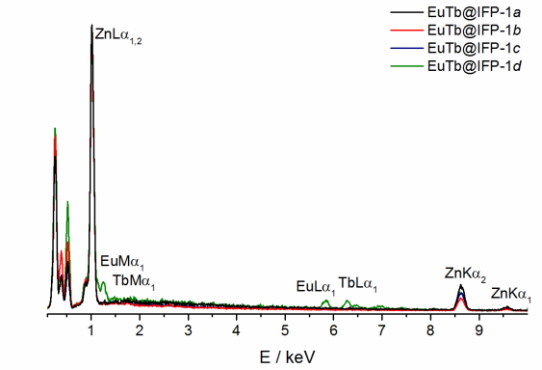

Fig. S07. Comparison of representative EDX-spectra of EuTb@IFP-1*a* (black), EuTb@IFP-1*b* (red); EuTb@IFP-1*c* (blue); EuTb@IFP-1*d* (green). All spectra are normalized to the $ZnL\alpha_{1,2}$ signal.

4 Elemental Mapping

Eu@IFP-1

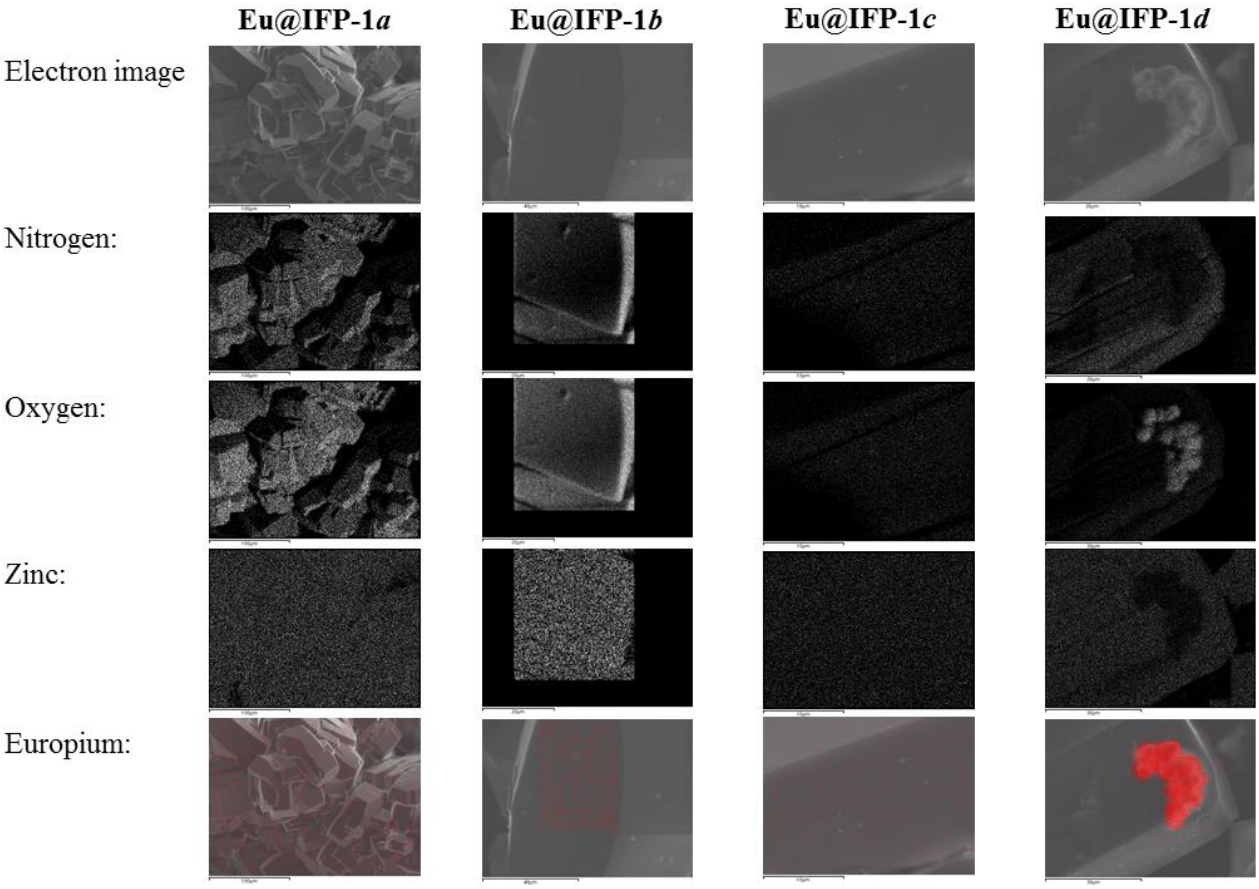

Fig. S08. Elemental mapping for Eu@IFP-1*a* - *d*.

Tb@IFP-1

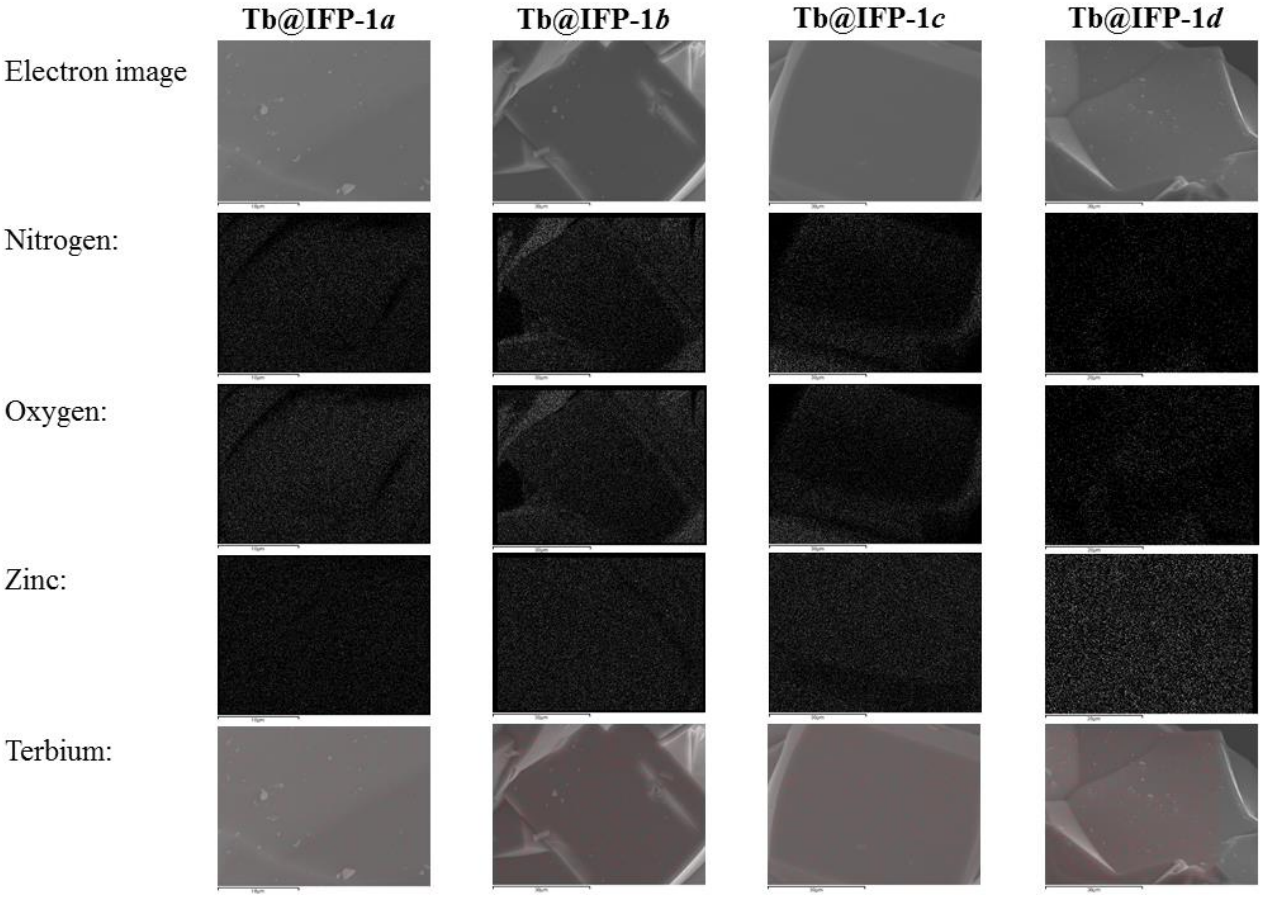

Fig. S09. Elemental mapping for Tb@IFP-1*a* - *d*.

EuTb@IFP-1

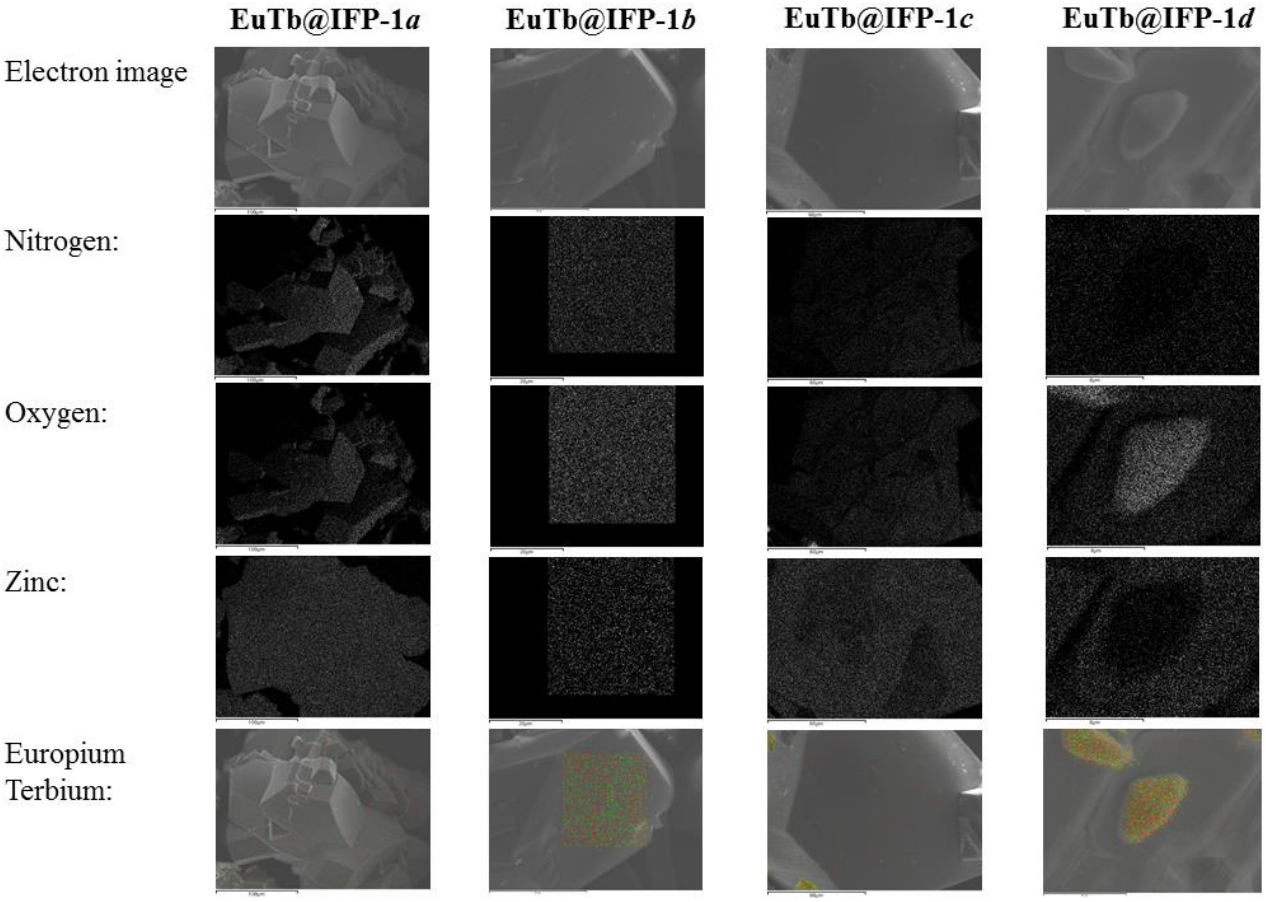

Fig. S10. Elemental mapping for EuTb@IFP-1*a* - *d*.

5 Thermogravimetric analysis (TGA)

TG measurements was performed in a static air atmosphere from room temperature up to 900 °C with a Perkin Elmer TGA 4000 thermal analyzer. The heating rate was 10 °C min^{-1}. The samples were placed in ceramic pans. TG-MS measurements were performed with Linseis STA PT-1600 online coupled mass spectrometer Pfeiffer MS Thermostar.

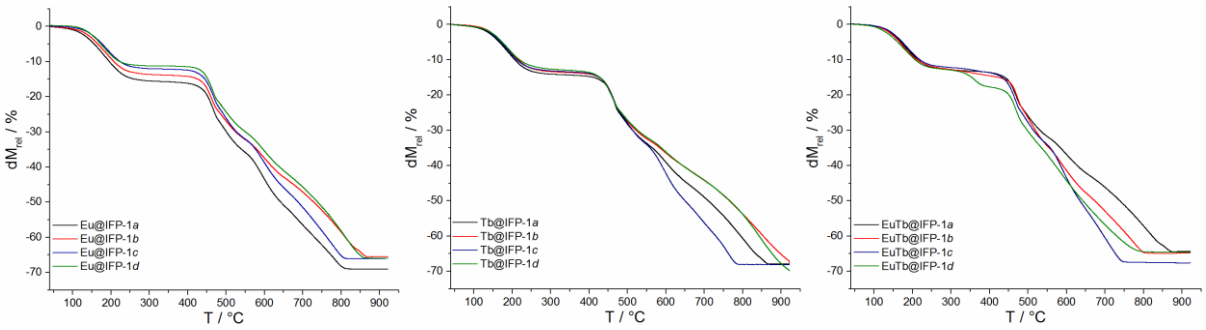

Fig. S11. TG curves of Ln@IFP-1 materials.

Thermogravimetric analyses (TGA) of as-synthesized IFP-1,[1] single-co-doped Eu@IFP-1*a* - *d* and Tb@IFP-1*a* - *d* as well as double-co-doped EuTb@IFP-1*a* - *c* containing an Ln-content lower than 1 atom% show a mass loss between 10-15 % in the first step up to 250 °C (Fig. S11, some examples). This can be attributed to the removal of water and DMF molecules, trapped in the pores. A long plateau in the temperature range from 280 to 400 °C is observed in all cases, indicating a certain thermal stability in the absence of these guest molecules. TG-MS analyses were done for EuTb@IFP-1*b* and EuTb@IFP-1*d* to check the anions formate most reasonable coordination partners for the Ln^{3+} ion. For the activated EuTb@IFP-1*d* a mass signal of formate could be detected (Fig. S12) which additionally proved the formation of a mixed $EuTb(HCOO)_3$ side phase.

6 TG-MS Analysis

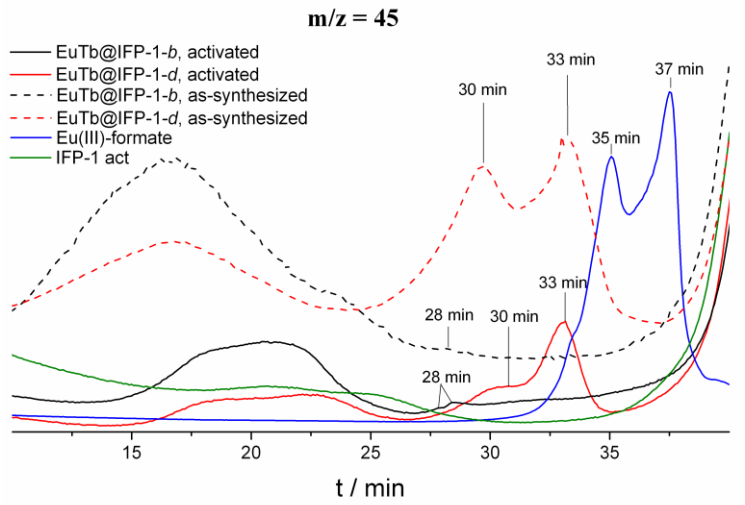

Fig. S12 Comparison of the mass signals of as synthesized, activated EuTb@IFP-1-*b* (black); as synthesized, activated EuTb@IFP-1-*d* (red); Eu(III)-formate (blue) and activated IFP-1 (green).

Table S04. Comparison of the mass signals (m/z = 45) for the as synthesized and activated compounds of EuTb@IFP-1-*b*, EuTb@IFP-1-*d*, activated IFP-1 and $Eu(HCOO)_3$.

MOF	Signal 1 [min]	Signal 2 [min]	Signal 3 [min]
EuTb@IFP-1-b as synthesized	8.5 – 26.7	28.4	—
EuTb@IFP-1-b activated	13.5 – 26.7	27.8	28.4
EuTb@IFP-1-d as synthesized	8.8 – 24.1	29.7	33.1
EuTb@IFP-1-d activated	14.1 – 26.5	30.3	33.2
IFP-1 activated	18.0 – 30.7	—	—
Eu(HCOO)3	—	35.1	37.5

7 Gas Sorption Measurements

All gas sorption experiments were carried out on a Quantachrome Autosorb AS-1C. N_2 (Linde Gas, purity > 99.999%) physisorption was determined at 77 K with dynamic p0-determination via a p0-cell at p = 760 mmHg. CO_2 (Linde Gas, purity > 99.999%) physisorption was determined at a setpoint of 195 K and fixed p0 value of 740 mmHg on an Oxford Instruments cryostat model Optistat MK1 with a customized sample cell holder assembly and an Oxford Instruments controller model ITC 503. Analysis and interpretation of data was done with the Quantachrome AS1Win software package, version 2.11. All measured samples were activated at 200 °C with pressures of $1 \cdot 10^{-3}$ mbar. IFP-1 in non-doped and doped states exhibit equilibration hindrances, which required extended equilibration times up to 60 min per analysis point. Even for N_2 as analyst gas prolonged equilibration was observed. All samples were heated in the outgas station, until outgassing rates were at least below 10 microns/minute in pressure increase and afterwards loaded with He (Linde Gas, purity > 99.999%) before analysis was carried out.

8 Photoluminescence and Decay Investigations

Photoluminescence measurements including excitation and emission spectra were recorded with a Horiba Yvon Jobin Fluorolog 3 equipped with a 450 W xenon-lamp, PMT detector and double grating monochromators for excitation and emission in Front-Face mode using spectroscopically pure quartz tubes. All spectra were corrected with correction spectra provided by the manufacturer and excitation spectra were measured with a photodiode reference detector. An edge filter (Reichmann Optik, GG400) were used when required.
Lifetimes determinations were performed with a Edinburgh Instrument FLSP920 spectrometer equipped with a 100 W Xenon µs flash lamp (µF920H), a 5 mW pulsed ps diode laser (λ_{max} = 376 nm) and double grated monochromators in Right-Angle mode. Lifetime determinations on ns-scale were fitted with IRF correction. On µs scale exponential tail fitting was used.
Room temperature time resolved emission spectra (TRES) were recorded using a wavelength tunable Nd:YAG-laser/OPO system (Spectra Physics/GWU) operated at 20 Hz as excitation light source and an intensified CCD camera (Andor Technology) coupled to a spectrograph (MS257 Model 77700A, Oriel Instruments) equipped with a 300 l/mm grating as detection system. The TRES were collected using the "box car" technique. The initial gate delay, δt, was set to 500 ns and the gate width was adjusted between 50 - 100 µs.
Luminescence measurements at 4 K were carried out by cooling the dry samples inside a copper sample holder placed in a vacuum chamber attached to the cold plate of a closed cycle liquid Helium cryostat. As excitation light source we used a narrow bandwidth (2 pm @ 500 nm) dye laser (Cobra Stretch, Sirah Laser –and Plasmatechnik, Kaarst, Germany) pumped by a 532 nm Nd:YAG Laser (Quanta Ray, Spectra Physics, Santa Clara, CA, USA). The repetition rate was set to 10 Hz with a pulse length of 8 ns. The laser dye Pyrromethane 597 (λ_{em} = 575 - 610 nm) was purchased from Sirah Laser- und Plasmatechnik (Kaarst, Germany). The excitation light was coupled into one of the branches of a Y-shaped fiber bundle while the other branch was connected to a spectrograph (Shamrock SR-303i, Andor Technology, Belfast, UK) equipped with an intensified CCD camera (iStar DH 720 18V 73, Andor Technology, Belfast, UK).

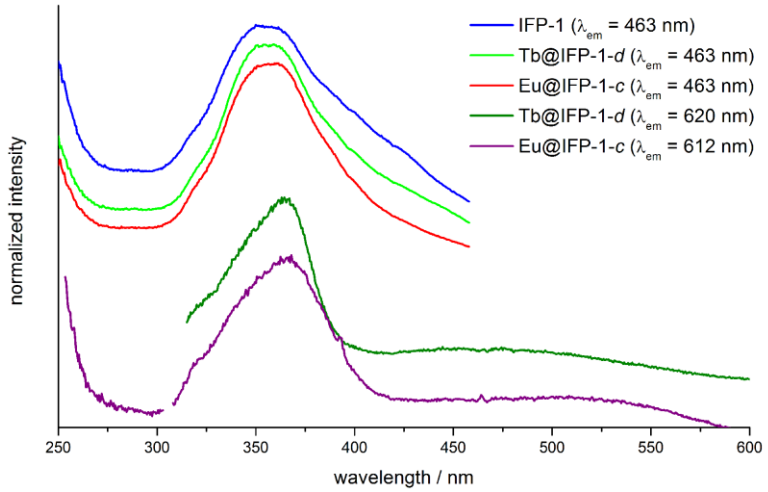

Fig. S13. Normalized excitation spectra of IFP-1 (blue), Eu@IFP-1-*c* (red, purple) and Tb@IFP-1-*f* (green, olive) for different relevant emission wavelengths.

Table S5. Chromaticity point coordinates x, y of IFP-1, EuTb@IFP-1b and EuTb@IFP-1d at room temperature and at 77 K (CIE 1931 standard).

MOF		Labeled in Fig.6 as	x	y
EuTb@IFP-1-d RT	as-synthesized,	(1)	0.315	0.371
EuTb@IFP-1-d 77K	as-synthesized,	(2)	0.271	0.258
EuTb@IFP-1-b RT	as-synthesized,	(3)	0.241	0.302
EuTb@IFP-1-b 77K	as-synthesized,	(4)	0.209	0.254
IFP-1		(5)	0.199	0.215

Table S6 Observed decay times (τ_{obs}) and χ^2 for IFP-1 as well as Eu@IFP-1*c* and Tb@IFP-1*d*.

Lifetime/ decay investigations					
Framework centered fluorescence			Ln-centered emission		
IFP-1			IFP-1		
λ_{ex} = 376 nm	λ_{em} = 470 nm	χ^2 = 1.694	-		
τ_{obs} (bi-exponential)	Lifetime (ns)	relative percentage (%)			
τ_1	0.33(1)	46			
τ_2	5.74(20)	54			
Tb@IFP-1*d*			Tb@IFP-1*d*		
λ_{ex} = 376 nm	λ_{em} = 470 nm	χ^2 = 1.917	λ_{ex} = 360 nm	λ_{em} = 543 nm	χ^2 = 1.246
τ_{obs} (bi-exponential)	Lifetime (ns)	relative percentage (%)	τ_{obs} (bi-exponential)	Lifetime (μs)	relative percentage (%)
τ1	0.04(2)	39	τ_1	580(33)	75
τ2	4.82(16)	61	τ_2	1062(60)	25
Eu@IFP-1*c*			Eu@IFP-1*c*		
λ_{ex} = 376 nm	λ_{em} = 470 nm	χ^2 = 1.347	λ_{ex} = 360 nm	λ_{em} = 615 nm	χ_2 = 1.026
τ_{obs} (bi-exponential)	Lifetime (ns)	relative percentage (%)	τobs (bi-exponential)	Lifetime (μs)	relative percentage (%)
τ_1	0.13(1)	28	τ_1	314(3)	73
τ_2	4.22(14)	72	τ_2	1337(117)	27

9 References

1 Debatin, F.; Thomas, A.; Kelling, A.; Hedin, N.; Bacsik, Z.; Senkovska, I.; Kaskel, S.; Junginger, M.; Müller, H.; Schilde, U.; Jäger, C.; Friedrich, A.; Holdt, H.-J. *Angew. Chem. Int. Ed.* **2010**, *49*, 1258.